BIOCHEMISTRY
including biophysical chemistry & molecular biology

Article

pubs.acs.org/biochemistry

Split Electron Paramagnetic Resonance Signal Induction in Photosystem II Suggests Two Binding Sites in the S_2 State for the Substrate Analogue Methanol

Johannes Sjöholm, Guiying Chen, Felix Ho, Fikret Mamedov, and Stenbjörn Styring*

Molecular Biomimetics, Department of Chemistry, Ångström Laboratory, Uppsala University, P. O. Box 523, SE-751 20 Uppsala, Sweden

ABSTRACT: Illuminating a photosystem II sample at low temperatures (here 5−10 K) yields so-called split signals detectable with continuous wave-electron paramagnetic resonance (CW-EPR). These signals reflect the oxidized, deprotonated radical of D1-Tyr161 ($Y_Z^{\bullet}$) in a magnetic interaction with the $CaMn_4$ cluster in a particular S state. The intensity of the split EPR signals are affected by the addition of the water substrate analogue methanol. This was previously shown by the induction of split EPR signals from the S_1, S_3, and S_0 states [Su, J.-H. et al. (2006) *Biochemistry 45*, 7617−7627.]. Here, we use two split EPR signals induced from photosystem II trapped in the S_2 state to further probe the binding of methanol in an S state dependent manner. The signals are induced with either visible or near-infrared light illumination provided at 5−10 K where methanol cannot bind or unbind from its site. The results imply that the binding of methanol not only changes the magnetic properties of the $CaMn_4$ cluster but also the hydrogen bond network in the oxygen evolving complex (OEC), thereby affecting the relative charge of the S_2 state. The induction mechanisms for the two split EPR signals are different resulting in two different redox states, $S_2Y_Z^{\bullet}$ and $S_1Y_Z^{\bullet}$ respectively. The two states show different methanol dependence for their induction. This indicates the existence of two binding sites for methanol in the $CaMn_4$ cluster. It is proposed that methanol binds to Mn_A with high affinity and to Mn_D with lower affinity. The molecular nature and S-state dependence of the methanol binding to each respective site are discussed.

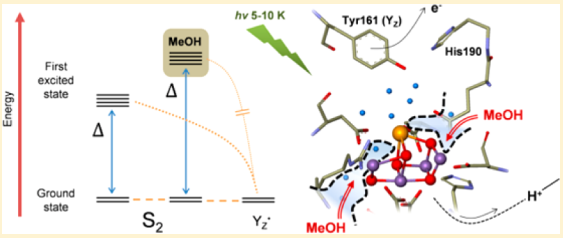

A key reaction in photosynthesis is the oxidation of water by photosystem II (PSII). The process is initiated by the light-induced charge separation at the chlorophyll array of P_{680}. An electron is transferred through the acceptor side cofactors, Pheo, Q_A and Q_B, leaving P_{680}^{+} which is oxidizing enough to ultimately extract electrons from water.[1−3] The water oxidation reaction takes place on the donor side of PSII at a catalytic center composed of four Mn ions and one Ca ion, bridged by O atoms.[4] For each molecule of oxygen produced, the $CaMn_4$ cluster cycles through five discrete redox states denoted S states ($S_n \rightarrow S_{n+1}$, $n = 0-4$). Oxygen is evolved in the $S_3 \rightarrow (S_4) \rightarrow S_0$ transition, where S_4 is a transient state, regenerating the most reduced state S_0. The S_1 state is the dominant state in the dark. The S_2 and S_3 states are metastable states that can be obtained from a dark-adapted PSII sample in the S_1 state after one or two short laser flashes, respectively.[5−7]

The electrons extracted from the $CaMn_4$ cluster are not transferred directly to P_{680}^{+} but are shuttled via a tyrosine residue, D1-Tyr161 (Y_Z).[8] Proton-coupled electron transfer takes place during this process. First, Y_Z is oxidized by P_{680}^{+} upon which its phenol proton is simultaneously transferred to the nearby base D1-His190,[4,9,10] thereby leaving a neutral radical ($Y_Z^{\bullet}$). Second, $Y_Z^{\bullet}$ is reduced by electron transfer from the $CaMn_4$ cluster and the phenol proton is regained from the histidine. Over the years, the importance of this proton coupled electron transfer reaction for an efficient donor side function of PSII has become increasingly clear.[11] The $CaMn_4$ cluster, its amino acid ligands, and Y_Z comprise the oxygen evolving complex (OEC) in PSII (as defined here).

Y_Z can be oxidized by illumination even at liquid helium temperatures.[12,13] As all S state transitions are completely inhibited below 77 K,[14] the fast rereduction of $Y_Z^{\bullet}$ from the $CaMn_4$ cluster (microsecond to millisecond at ambient temperature) is blocked. Instead $Y_Z^{\bullet}$ is reduced in the minutes time scale, in most cases via recombination with Q_A^{-}.[12] The $Y_Z^{\bullet}$ radical may interact magnetically with the $CaMn_4$ cluster in the different S states and can be observed with electron paramagnetic resonance (EPR) at 5−20 K as a broadened radical signal. These are the so-called split EPR signals from $S_nY_Z^{\bullet}$. The spectral appearance of the interaction signal is dependent on the redox state of the intact cluster and has in several aspects served as a valuable tool to study the donor side reactions in PSII (see refs 12 and 13 and references therein). In the present work, split EPR signals induced with the $CaMn_4$ cluster poised in the S_2 state are used to probe the interaction of the substrate analogue methanol to the OEC.

Since the catalytic activity of PSII requires an aqueous environment it has not been a trivial task to analyze substrate

Received: February 5, 2013
Revised: April 24, 2013
Published: April 26, 2013

   dx.doi.org/10.1021/bi400144e | *Biochemistry* 2013, 52, 3669−3677

water interactions in the OEC.[15] Waters binding to and reacting at the $CaMn_4$ cluster must be distinguished from waters that are present but not otherwise directly participating in the water oxidation reaction. Therefore, many substrate analogues such as different amines, hydrazine, hydrogen peroxide, hydrogen sulfide, and several alcohols have been used to explore substrate binding to the $CaMn_4$ cluster.[16,17]

Among the different substrate analogues, methanol is thought to coordinate directly to at least one of the Mn ions in the cluster in the S_2 state,[18,19] and candidates for the methanol binding Mn ion have been proposed based on structural modeling, spectroscopic investigations, and theoretical analysis.[20,21] Interestingly, methanol changes the shape and/or intensity of essentially all known continuous wave-electron paramagnetic resonance (CW-EPR) signals from the OEC, including the split EPR signals and the S_0 and S_2 multiline EPR signals (see ref 22 and references therein). Previously, the binding of methanol was investigated in an S state dependent manner by following the effects of methanol on both the S_0 and S_2 state multiline EPR signals[23] and the split EPR signals induced from the S_0, S_1, and S_3 states.[22]

In this paper, the methanol dependence of two split EPR signals induced from the S_2 state are investigated, thereby completing the set of experimental data across the S states. By this, a comprehensive depiction of the effect of methanol on the discrete S states is achieved. The results imply that methanol coordinates to two distinct sites at the $CaMn_4$ cluster in the S_2 state and that the binding not only affects the magnetic properties of the cluster but also the protonation state in the OEC, affecting the relative charge of the S_2. The molecular identity of each respective site is discussed.

MATERIALS AND METHODS

PSII Membrane Preparation. PSII-enriched membranes (BBY type) were prepared from hydroponically grown spinach (*Spinacia oleracea*).[24,25] The steady state oxygen evolution activity from the preparation was ~350 μmol of O_2 mg of Chl^{-1} h^{-1} when measured under saturating light conditions with a Clark-type electrode. The measurement was performed at 20 °C in a buffer with 25 mM MES-NaOH (pH 6.3), 10 mM NaCl, 5 mM $MgCl_2$, 5 mM $CaCl_2$ and 400 mM sucrose at ~20 μg of Chl/mL using 0.5 mM P*p*BQ (in DMSO) as an electron acceptor. Chl concentrations were determined according to ref 26. The preparation was kept at −80 °C in a buffer containing 25 mM MES-NaOH (pH 6.3), 15 mM NaCl, 3 mM $MgCl_2$, and 400 mM sucrose.

Synchronization of the OEC and Preparation of the S_2 State. The PSII membrane preparation with a concentration of ~2.5 mg of Chl/mL was put into calibrated EPR tubes. A methanol and water mixture was added with a precision syringe to reach the desired final concentration (0−5% v/v).[22] All samples were exposed to room light for 5 min to fully oxidize Y_D and then dark adapted for 30 min. The PSII samples were synchronized in the dark-stable S_1 state by giving one preflash and then dark adapting for 15 min at 20 °C.[14,27] After dark adaptation P*p*BQ was added to a final concentration of 1 mM (from a 50 mM stock solution in DMSO). The S_2 state was achieved by giving 1 saturating turnover laser flash to the EPR sample equilibrated at 0 °C. Flashes were provided by a Nd:YAG laser (Spectra Physics, USA) at a frequency of 5 Hz (532 nm, 850 mJ/pulse).

EPR Spectroscopy. CW-EPR measurements were performed with a Bruker ELEXSYS E500 spectrometer using a SuperX EPR049 microwave bridge. Low-temperature experiments were carried out with a Bruker SHQ 4122 cavity equipped with an Oxford Instruments cryostat. Samples were cooled with liquid helium, and an Oxford ITC 503 temperature controller was used for fine temperature adjustments. Signal processing and quantification were carried out with the Bruker Xepr software. Spectrometer settings are given in the figure legends.

EPR Signal Induction and Analysis. The light-induced EPR signals were produced with illumination at 5−10 K. For visible light illumination, continuous white light was provided by a 150 W projector lamp fitted with a neutral density filter (10% T, Schott NG9). The light was filtered through a $CuSO_4$ solution and directed into the cavity using a Plexiglas light guide. The light intensity at the position of the cavity window was 20 W/m^2. For NIR illumination, light was provided at 830 nm by a continuous laser diode (LQC830-135E, Newport, USA). After passing through a beam spreader, the light intensity at the cavity window was 67 W/m^2. The quantification of the light-induced EPR signals was done by measuring the height of the peak, for the NIR induced signal, or trough, for the visible light induced signal, indicated in Figures 1−3. The intensity of the multiline EPR signal was measured as the peak height of six of the hyperfine peaks (indicated in Figures 4 and 5).

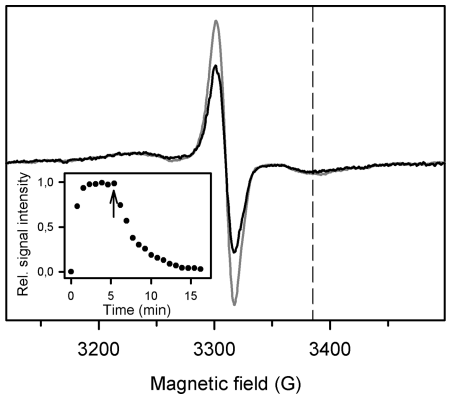

Figure 1. Induction of a split EPR signal from a sample in the S_2 state with visible light at 5 K in the presence of 5% methanol. The total light-induced signal (gray spectrum) is shown in a difference EPR spectrum between the spectrum recorded before illumination and the spectrum recorded during illumination (light-*minus*-dark), and the decaying part of the signal (black spectrum) was obtained by subtraction of a spectrum recorded after 15 min decay at in the dark at 5 K from the spectrum recorded during illumination (light-*minus*-post decay). In the latter spectrum long-lived radicals (e.g., Chl, Car) are not contributing to the EPR spectrum. The inset shows the induction of the split EPR signal during illumination and its subsequent decay in the dark after illumination was stopped (arrow) at 5 K measured at the field position indicated with a dashed line. EPR conditions: Microwave frequency 9.28 GHz, microwave power 25 mW, field modulation frequency 100 kHz, modulation amplitude 10 G, temperature 5 K.

In addition to the S_2 multiline EPR signal, the S_2 state can also exhibit another EPR signal in various amounts centered at $g \sim 4.1$, caused by minor structural differences between two states.[28] In the present experimental series, we did not observe the $g \sim 4.1$ signal, either in the presence or in the absence of methanol. This probably reflects subtle properties in the OEC due to our sample preparation and S state advancement

dx.doi.org/10.1021/bi400144e | *Biochemistry* 2013, 52, 3669−3677

procedure, which are interesting but outside the context of the present study.

RESULTS

The effect of the addition of methanol on the intensity of two split EPR signals was investigated. Both signals were induced from a PSII sample with the $CaMn_4$ cluster synchronized in the S_2 state. The split EPR signals were induced by illumination at liquid helium temperatures (5−10 K). One was induced by visible light illumination, and the other signal was induced by NIR (830 nm) illumination.

Effect of Methanol on the Split EPR Signal Induced with Visible Light Illumination. Ioannidis et al.[29] reported that a 160 G wide split EPR signal centered at 3310 G can be induced with visible light illumination at 10 K from a sample poised in the S_2 state in the presence of methanol. At a methanol concentration of 5%, a light-*minus*-dark difference spectrum (Figure 1, gray spectrum) resembles the previously reported signal.[29] The induction of the signal by continuous light illumination and its decay in the dark was followed at the high field trough at 3385 G (inset, Figure 1). The decay of the signal at 5 K was estimated to have a $t_{1/2} \sim 2$ min. As observed for all split EPR signals reported a narrow derivative signal was observed at $g \sim 2$ (3310 G). This part of the spectrum is complex and contains a fraction of light-induced Car and Chl radicals.[30] These radicals can be separated from the split EPR spectrum ($t_{1/2}$ ~2 min) as they are slowly decaying (hours) in the dark. By subtracting the signal recorded after 15 min decay in dark from the signal recorded during illumination, a spectrum representing the "pure" split EPR signal was obtained. This spectrum, shown in Figure 1 (black spectrum), still contains a derivative feature at 3310 G.

To investigate the methanol dependence of the signal in Figure 1, samples with varying methanol concentration were illuminated with visible light at 5 K. Figure 2A compares the 160 G split EPR signal induced in samples containing 5% (black spectrum) and 0.5% (gray spectrum) methanol. The signal intensity clearly decreased with decreasing methanol concentration. In contrast, the spectral shape seemed not to be dependent on the methanol concentration. The split EPR signal amplitude was measured at 3385 G at methanol concentrations between 0 and 5% (Figure 2B). The maximal signal amplitude was reached between 1 and 2% methanol. The concentration where half of the spectral change has occurred is defined as $[MeOH]_{1/2}$[22,23] and is used here for comparing the observed effect of methanol with data from other S states. The $[MeOH]_{1/2}$, determined from the hyperbolic fit (Figure 2B, dashed line), was 0.28 ± 0.03%.

Effect of Methanol on the Split EPR Signal Induced with NIR Light Illumination. By illuminating a sample in the S_2 state with NIR light at liquid helium temperature a different split EPR signal could be induced (Figure 3A).[31] In the absence of methanol, the signal intensity of this split EPR signal slowly increased to a maximum with continuous 830 nm light illumination at 10 K (inset Figure 3A). The signal did not decay in the dark after illumination was stopped as is usually seen with split EPR signals induced with visible light.[30,32−34] Subtracting the spectrum before illumination from the spectrum recorded after 20 min NIR light illumination at 10 K yielded the light-*minus*-dark difference spectrum shown in Figure 3A (black spectrum). The signal has a positive peak at 3280 G and a small derivative feature at 3340 G.

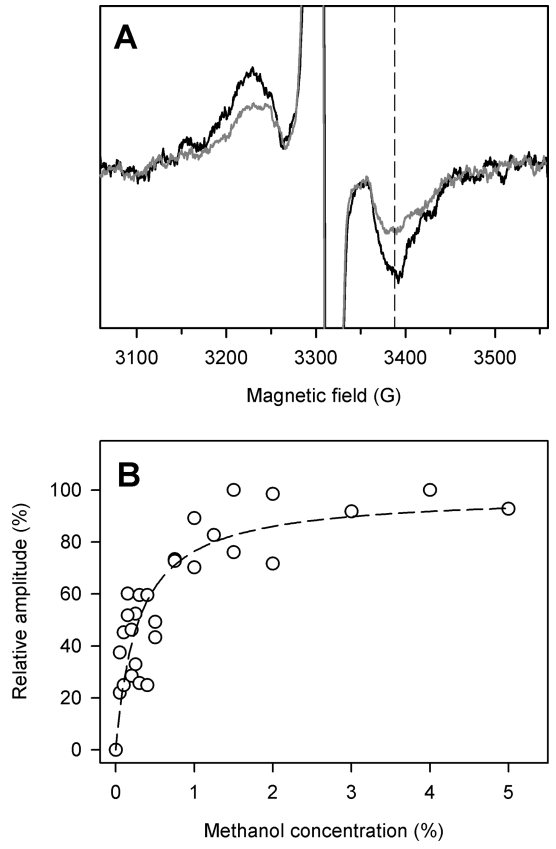

Figure 2. Methanol dependence of the visible light induced split EPR signal. (A) Spectra of the split EPR signal induced with visible light illumination at 5 K in the presence of 5% (black spectrum) or 0.5% (gray spectrum) methanol. The spectra shown are light-*minus*-dark difference spectra. (B) The amplitude of the split EPR signal recorded in samples with 0−5% methanol concentration. The amplitude was measured at 3385G (indicated with a dashed line in panel A). EPR conditions: Microwave frequency 9.28 GHz, microwave power 25 mW, field modulation frequency 100 kHz, modulation amplitude 10 G, temperature 5 K.

The effect of methanol on this NIR-induced split EPR signal was investigated by following the change in signal amplitude as a function of methanol concentration. The signal decreased with increasing concentrations of methanol and already at 0.1% methanol almost 50% of the signal amplitude was lost (Figure 3A, gray spectrum). Figure 3B shows the methanol dependence of the signal intensity between 0 and 5%, and there is essentially no observable split EPR signal >1% methanol. The $[MeOH]_{1/2}$, determined from a hyperbolic decay fit of the data points (Figure 3B, dashed line), was 0.10 ± 0.01%.

Methanol Effects on the S_2 Multiline EPR Signal. The S_2 state of the $CaMn_4$ cluster gives rise to a characteristic EPR signal known as the S_2 multiline EPR signal (Figure 4A). The S_2 multiline EPR signal is affected by methanol and differs in, e.g., resolution of hyperfine structure, total width of hyperfine pattern, and microwave power saturation behavior between treated and nontreated samples (see, e.g., refs 23 and 35). Most notably, the intensity of the multiline EPR signal has been shown to increase with increasing methanol concentration.[23] This was investigated in the samples used here for split EPR signal induction by measuring the amplitude of the multiline EPR signal as a function of methanol concentration.

dx.doi.org/10.1021/bi400144e | *Biochemistry* 2013, 52, 3669−3677

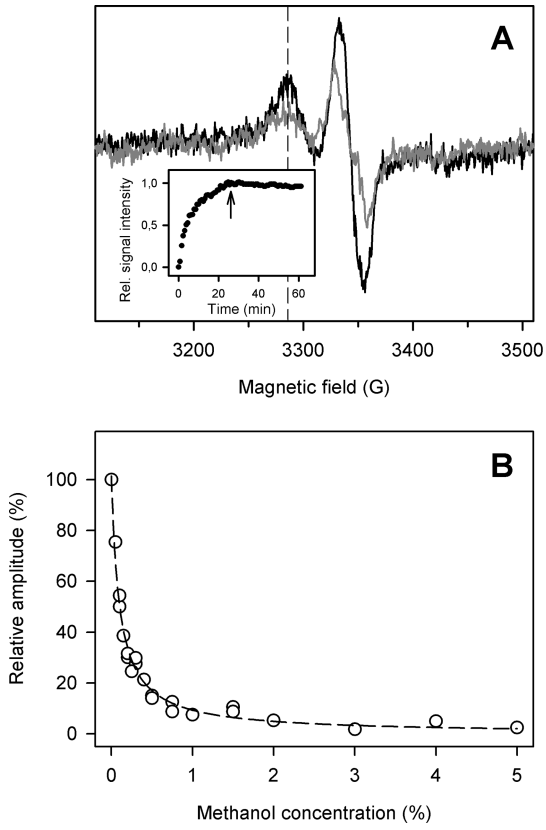

Figure 3. Induction and methanol dependence of the split EPR signal induced with NIR illumination of a sample in the S_2 state at 10 K. (A) Spectra representing the split EPR signal produced by illumination at 830 nm at 10 K in the absence of methanol (black spectrum) or in the presence of 0.1% methanol (gray spectrum). The spectra are obtained by subtracting the spectrum recorded in dark from the spectrum recorded after 20 min continuous illumination. The inset shows the amplitude of the split EPR signal during continuous illumination with 830 nm light and after the illumination was stopped (arrow). The change in signal amplitude was measured at 3240 G (indicated with a dashed line) (B) Methanol dependence of the NIR-induced split EPR signal in samples with 0−5% methanol concentration. The split EPR signal was induced by continuous 830 nm illumination for 20 min, and the amplitude was measured at 3240 G. The maximum signal intensity, measured at 0% methanol, was set as 100%. EPR conditions: Microwave frequency 9.28 GHz, microwave power 25 mW, field modulation frequency 100 kHz, modulation amplitude 10 G, temperature 10 K.

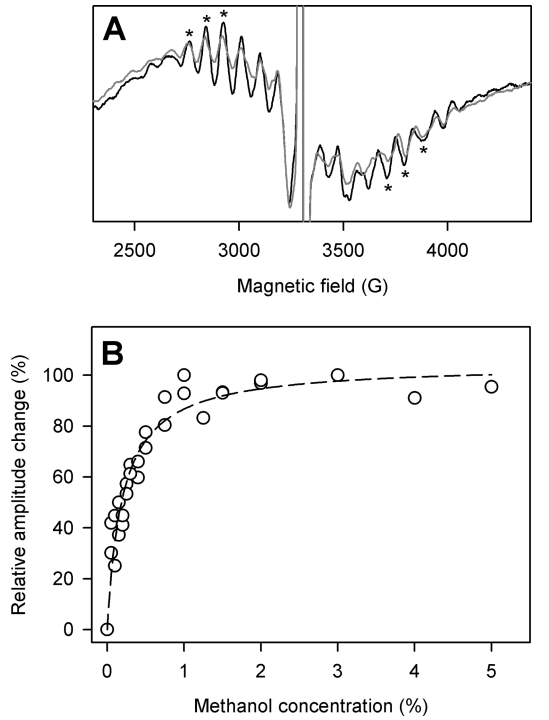

Figure 4. Methanol dependence of the S_2 state multiline EPR signal. (A) The S_2 multiline EPR signal recorded at 10 K in a sample containing 0% (gray spectrum) or 5% (black spectrum) methanol. (B) Methanol induced relative amplitude change of the S_2 multiline EPR signal. The methanol-induced change of the signal amplitude relative to the signal amplitude in the sample with 0% methanol is shown. The maximal amplitude change is set as set as 100%. The signal amplitude is estimated at the field positions marked with asterisks in panel A. EPR conditions: Microwave frequency 9.28 GHz, microwave power 10 mW, field modulation frequency 100 kHz, modulation amplitude 20 G, temperature 10 K.

Figure 4B shows the methanol-induced change of the signal amplitude relative to the signal amplitude without methanol (i.e., the multiline signal amplitude in the 0% methanol sample). At the maximal amplitude change (set as 100%), the multiline EPR signal was approximately double that of a sample without methanol addition. This is depicted in Figure 4A, where the multiline EPR signal from samples containing 5% (Figure 4A, black spectrum) and 0% (Figure 4A, gray spectrum) methanol is compared. The value of $[MeOH]_{1/2}$ for the amplitude increase of the S_2 multiline EPR signal was 0.20 ± 0.03% determined from a fitting of the data points using a hyperbolic function (Figure 4B, solid line).

During the induction of both the visible and NIR-induced split EPR signals, a reduction in the intensity of the S_2 multiline EPR signal was observed here. This has also been reported previously.[29,36] During visible light illumination in the presence of methanol the intensity of the multiline EPR signal decreased with approximately 25% (results not shown). During NIR illumination in the absence of methanol, the intensity of the S_2 multiline EPR signal decreased with 22% (results not shown).

However, as shown in Figure 5, even in the presence of 5% methanol, where no NIR-induced split EPR signal was observed (see Figure 3), the intensity of the multiline EPR signal decreased during illumination at 10 K. This is easily observed from the negative peaks of the multiline EPR spectrum after a light-*minus*-dark subtraction (Figure 5). In this difference spectrum, it can also be seen that no split EPR signal was induced during NIR illumination in the presence of methanol. The decrease in the intensity of the multiline EPR signal during illumination was quantified to approximately 13% of the total intensity. We did not observe any change in the width of the hyperfine peaks during illumination that could account for this decrease. This was verified by a simple normalization and comparison of the spectra before and after illumination.

As shown previously in the absence of methanol, the S_2 multiline EPR signal intensity (as well as the intensity of the NIR induced split EPR signal) is stable in the dark after illumination.[36] This was also the observed behavior here in the presence of 5% methanol; i.e., the intensity of the multiline EPR signal did not recover during dark incubation at 10 K after the illumination was stopped (results not shown).

dx.doi.org/10.1021/bi400144e | *Biochemistry* 2013, 52, 3669−3677

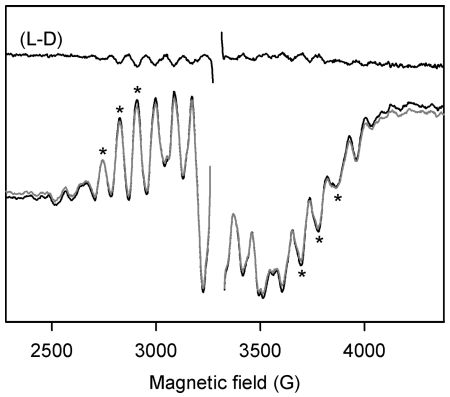

Figure 5. Decrease of the intensity of the S_2 state multiline EPR signal during NIR illumination. The S_2 multiline EPR signal in a sample with 5% methanol was recorded before (black spectrum) and during (gray spectrum) illumination with NIR light at 10 K. The change in multiline EPR signal intensity is highlighted by the light-*minus*-dark difference spectrum at the top in the panel (L-D; light-*minus*-dark). EPR conditions: Microwave frequency 9.28 GHz, microwave power 10 mW, field modulation frequency 100 kHz, modulation amplitude 20 G, temperature 10 K.

DISCUSSION

The Effect of Methanol in the S_2 State. Two split EPR signals induced from the S_2 state are here used to characterize S-state dependent methanol effects in photosystem II. Interestingly, methanol affects the two signals differently; one disappears in the presence of methanol (Figure 3), while the other appears with the addition of methanol (Figure 2).

Without methanol, a split EPR signal is induced by illumination with NIR light at 10 K. It has been suggested that this signal originates from a $S_1Y_Z^\bullet$ state formed via an electron transfer from Y_Z back to the S_2 state induced by excitation of Mn.[31,36] In the presence of methanol however, the split EPR signal from the $S_1Y_Z^\bullet$ state is not observed upon NIR illumination. There are two possible reasons for this; either the NIR sensitivity of the $CaMn_4$ cluster is lost in the presence of methanol and the $S_1Y_Z^\bullet$ state is not induced at all, or the $S_1Y_Z^\bullet$ state is formed but the interaction is not observable with EPR. At this point, we favor the second explanation. This is supported by the loss of multiline EPR signal intensity independent of the presence of methanol (Figure 5).[31,36] A loss of multiline EPR signal intensity upon light illumination can be accounted for by the NIR promoted reaction $Mn^*S_2Y_Z \rightarrow MnS_1Y_Z^\bullet$, thus decreasing the S_2 centers giving rise to the multiline EPR signal.

The lack of an EPR detectable $S_1Y_Z^\bullet$ split signal can instead be explained by the changed electronic configuration of the $CaMn_4$ cluster in the presence of methanol. Methanol is postulated to increase the Mn to Mn exchange coupling in the cluster and thereby increase the ground to first excited state energy-level difference.[21,37−41] In the S_1 state, the split EPR signal has been attributed to the interaction between the first excited state $S = 1$ of the $CaMn_4$ cluster and the $S = 1/2$ of $Y_Z^\bullet$.[22,42] In the presence of methanol, Su et al. suggested that the excited spin would be moved out of thermal reach at 5−10 K,[22] and consequently, even though $Y_Z^\bullet$ is formed by NIR illumination, the split EPR signal is not observed.

In contrast to above, a split EPR signal is induced in the presence of methanol when illuminating with visible light at 5 K. This signal has been assigned to a $S_2Y_Z^\bullet$ state induced via the reaction $S_2Y_Z\ P_{680}{}^+Q_A{}^- \rightarrow S_2Y_Z^\bullet\ P_{680}Q_A{}^-$.[29] Following the reasoning of Su et al.,[22] the $S_2Y_Z^\bullet$ split EPR signal is likely to originate from the ground state $S = 1/2$ of the $CaMn_4$ cluster and not from an excited state. This is also supported by the decrease of the S_2 state multiline EPR signal observed here and in ref 29 as it has been suggested that if the $S = 1/2$ of the $CaMn_4$ cluster is in a magnetic interaction with $Y_Z^\bullet$, it would no longer contribute to the intensity of the multiline EPR signal.[22,29]

However, when illuminating with visible light in the absence of methanol the $S_2Y_Z^\bullet$ split EPR signal is not observed. This contrasts the behavior of the split EPR signal induced with visible light from the S_0 state ("the split S_0 EPR signal") reported in ref 22, also suggested to originate from the ground state $S = 1/2$ of the $CaMn_4$ cluster. This signal is observed independently of the presence of methanol (though showing a spectral change).

What is then the reason for the lack of $S_2Y_Z^\bullet$ induction without methanol? Previously, this has been associated with the charge of the $CaMn_4$ cluster in the S_2 state.[13,29,36] At ambient temperature, Y_Z has been suggested to function as an electrostatic promoter,[7,43−45] and $Y_Z^\bullet$ formation in the S_2 state then causes a shift of p*K* values at the Mn cluster and the concomitant release of one proton before Mn oxidation to reach the S_3 state.[7,46] At 5 K, this proton release is considered to be blocked, and the resulting extra charge of the $CaMn_4$ cluster hinders a stable formation of the $Y_Z^\bullet$ − D1-His190$^+$ pair (see discussion in ref 36). To observe the $S_2Y_Z^\bullet$ state with EPR, the charge of the cluster must first be lowered.[a]

Hence, the induction of the $S_2Y_Z^\bullet$ signal in the presence of methanol indicates that the $Y_Z^\bullet$ − D1-His190$^+$ pair can be stably formed in order for the EPR signal to be observed at 5 K. This is interesting and implies that methanol either (i) lowers the charge of the cluster when binding or (ii) promotes a lowering of the charge upon illumination at 5 K. The second point however entails a proton movement at the temperature of split EPR signal induction. Regardless, the results presented here show that methanol not only changes the apparent electronic properties of the $CaMn_4$ cluster but could also invoke a indirect effect on the protonation state and/or the hydrogen bond network within the OEC by its way of coordinating to the cluster (e.g., by replacing a Mn ligand). The remaining of this discussion will deal with the mode of methanol binding and the possible binding sites in the OEC.

One or Two Sites for Methanol Binding at the CaMn4 Cluster. There are numerous investigations of methanol effects on PSII properties like O_2 evolution,[18,23,47] miss factors,[47] EPR signals (Table 1), ENDOR and ESEEM spectra.[18,19,21,35] In cases where the concentration dependence has been studied, the effect has been possible to explain by invoking one binding site for methanol. However, by reviewing the literature (Table 1), it can be noted that while the $[MeOH]_{1/2}$ values reported for the EPR signals originating from the S_1 state of the $CaMn_4$ cluster are always low, ranging from 0.10 to 0.12%, the EPR signals originating from the S_2 state range from 0.20 to 0.35%. In the S_0 and S_3 states, the $[MeOH]_{1/2}$ was even higher. Such differences might indicate the existence of multiple sites for methanol, having different binding affinities (reported as $[MeOH]_{1/2}$ in Table 1).

The possibility of multiple sites was first addressed in our earlier compilation of methanol binding data that was combined with a computer modeling approach to analyze channels and binding sites to the OEC.[20,22] In that work, where

dx.doi.org/10.1021/bi400144e | *Biochemistry* 2013, 52, 3669−3677

Table 1. Methanol Dependence of the Different EPR Signals from the OEC

starting S state	EPR signal	$[MeOH]_{1/2}$ % (v/v)	$[MeOH]_{1/2}$ mM	effect on EPR signal	ref
S_1	$S_1Y_Z^{\bullet}$[a] (split S_1)	0.12 ± 0.05	30	decreases	22
	S_1 $g \sim 4.9$	nr[d]		decreases	37
S_2	$S_1Y_Z^{\bullet}$[b]	0.10 ± 0.01	25	decreases	this work
	$S_2Y_Z^{\bullet}$[a]	0.28 ± 0.03	69	increases	this work
	S_2 multiline	0.20 ± 0.03; 0.35 ± 0.08	49; 86	increases	this work[23]
	S_2 $g \sim 4.1$	0.20 ± 0.08	49	decreases	23
S_3	$S_2'Y_Z^{\bullet}$[c] (split S_3)	0.57 ± 0.05	141	decreases	
	S_3 $g \sim 8, 12$	nr[d]		decreases	48, 49
S_0	$S_0Y_Z^{\bullet}$[a] (split S_0)	0.54 ± 0.05	133	modified/ increases	22
	S_0 multiline	0.40 ± 0.07	99	increases	23

[a]Induced at 5 K with visible light illumination. [b]Induced at 10 K with 830 nm light from a sample poised in the S_2 state. A reduction of the $CaMn_4$ cluster upon NIR illumination is suggested to yield a S_1 state. [c]Induced at 5 K with 830 nm light from a sample poised in the S_3 state. NIR illumination is suggested to yield a S_2' state, the prime indicates a possibly modified, deprotonated S_2 state [d]Not reported.

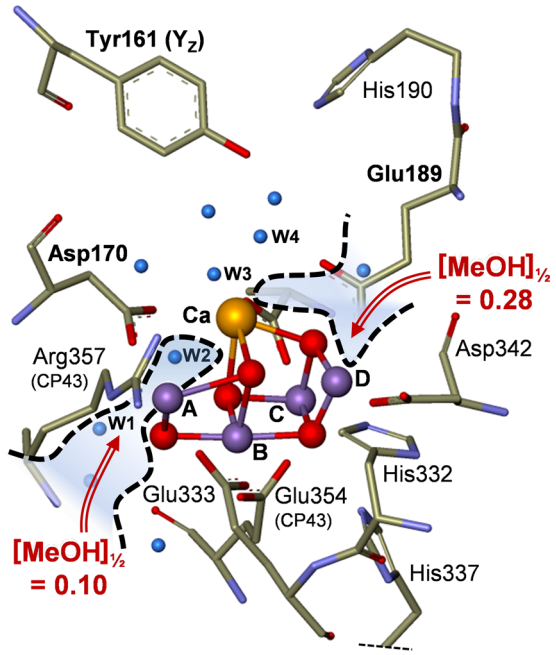

Figure 6. Illustration of the two suggested methanol binding sites in the OEC from the 1.9 Å resolution structure.[4] The low affinity site for methanol is located at Mn_D where the carboxyl group of D1-Glu189 is displaced. The high affinity site is located at Mn_A where methanol probably dislocates one of the OH ligands. Water positions found in the structure are indicated with blue balls, and the four water molecules that coordinate to the $CaMn_4$ cluster are labeled W1–W4. The Mn ions A, B, C, and D (our nomenclature) correspond to Mn4, Mn3, Mn2, and Mn1, respectively, as labeled in ref 4. The figure was prepared from PDB ID: 3ARC.

the structural analysis was based on the medium-resolution X-ray structure of PSII,[50] two of the Mn ions (Mn_A and Mn_B in Figure 6) were implicated to be potential methanol binding sites. It was also pointed out that methanol could access D1-Glu189 that coordinates both Ca and Mn_D (Figure 6). Despite this, the methanol binding was interpreted with a model where methanol coordinates to one Mn ion, and different affinities in the various S states were rationalized[20,22] by the structural changes in the $CaMn_4$ cluster that occur during the $S_2 \rightarrow S_3 \rightarrow S_0$ transitions.[51,52]

In light of our present data, this interpretation seems oversimplified, keeping in mind that no structural changes are considered to be involved in the $S_1 \rightarrow S_2$ transition. From our determined values of $[MeOH]_{1/2}$, we find evidence for two binding sites of methanol, at least in the S_2 state (see further below). At low methanol concentrations ($[MeOH]_{1/2}$ = 0.10%), the $S_1Y_Z^{\bullet}$ EPR signal disappears when induced by NIR illumination at 10 K. Since methanol will not bind or unbind at 10 K, the observed $[MeOH]_{1/2}$ reflects binding to a site that must exist in the S_2 state. We denote this the high affinity site. From earlier work, it also seems clear that the same site exists also in the S_1 state since the $S_1Y_Z^{\bullet}$ EPR signal decreases with the same methanol dependence when the S_1 state is illuminated with visible light at 10 K (Table 1). Thus, methanol in this high affinity site influences EPR signals from the S_1 state in the same way, irrespective of whether S_1 was formed by dark incubation of PSII at room temperature or by NIR illumination of the S_2 state at ultralow temperature (10 K).

However, methanol also binds to a site with a higher $[MeOH]_{1/2}$. This is observed here as the appearance of the $S_2Y_Z^{\bullet}$ EPR signal ($[MeOH]_{1/2}$ = 0.28%) and the increased intensity of the S_2 multiline EPR signal ($[MeOH]_{1/2}$ = 0.20%). In fact, methanol in this site affects all EPR signals that reflect the $CaMn_4$ cluster being in the S_2 state (Table 1). We denote this the low affinity site. Importantly, at concentrations when methanol is bound at the low affinity site (affecting the S_2 state EPR signals), it is also bound to the high affinity site. It is probable that this has implications for earlier interpretations of ESEEM spectra[18,19] in the presence of methanol (discussed below).

Further, available data indicate that the low affinity site also exists in the S_1 state. This can be concluded since methanol exerts the same effect on the spectral shape of the S_2 state multiline EPR signal irrespective if this is formed by 1 flash (ref 23 and the present work) or by illumination of a S_1 state sample at 200 K.[19,35] It is furthermore probable that this site also exists in the S_0 state where the studied probes, the split S_0 EPR signal and the S_0 state multiline EPR signal both show elevated $[MeOH]_{1/2}$ values (0.54% and 0.40% respectively; Table 1). As earlier proposed by Åhrling et al.,[19] the increase in the S_0 multiline EPR signal with increasing methanol concentration probably has the same mechanistic origin as the increase in the S_2 multiline EPR signal indicating binding to the same Mn ion. However, in the S_0 state (as well as in the S_3 state) structural changes possibly also influence the apparent binding affinities as compared to the S_1 and S_2 states.

Taken together, the results indicate the presence of two binding sites for methanol in the OEC. We find the alternative, that methanol can recoordinate leading to the observation of different binding affinities at the temperature of the experiments (5–10 K), unlikely. Furthermore, the results indicate that the low affinity site is available in all S states. In contrast, the high affinity site has so far only been observed in the S_1 and S_2 states. At present, this site has not been studied in the S_3 and S_0 states due to lack of experimental probes.

dx.doi.org/10.1021/bi400144e | Biochemistry 2013, 52, 3669–3677

Nature of the Two Binding Sites. Where are these sites located in the $CaMn_4$ cluster and which Mn ions are involved? The best studied and most discussed site is the low affinity site that affects the S_2 multiline EPR signal. Here, direct binding of methanol to Mn has been proven by spectroscopic studies using isotope labeled methanol. Very detailed suggestions about this site were made by Åhrling et al.[19,35] On the basis of ESEEM and EPR studies, it was concluded that methanol was bound to a Mn(III) ion in the S_2 state. This Mn ion was probably 5-coordinated in the absence of methanol, although it was not excluded that methanol in fact displaced a protein ligand to the Mn ion. Presently, it is believed that there is only one Mn(III) ion in the S_2 state,[53] and it has been suggested to be Mn_D in Figure 6.[54−56]

The methanol binding to the S_2 state was recently revisited by Su et al.[21] where the ESEEM data from refs 18 and 19 were used together with the structural model for the $CaMn_4$ cluster in the S_2 state derived by Siegbahn.[57] The authors argued that Mn_D was one of four possible binding sites for methanol.[21] It was pointed out that methanol was unlikely to bind to the vacant site on the 5-coordinated Mn_D. Rather, the data from Åhrling et al.[19] instead were interpreted to favor displacement of the carboxyl-group of the D1-Glu189 ligand (Figure 6) which bridges Mn_D and the Ca ion (see discussion in ref 21). Methanol binding to this site would be coherent with the channel modeling work,[20] which indicated that methanol could have easy access to both the Ca ion and D1-Glu189.

However, it can be argued that displacement of a critical ligand like D1-Glu189 would have severe effects on the OEC. Still, exchange of D1-Glu189 for Gln, Lys, Arg, Leu, or Ile, that all will be unable to coordinate both Mn and Ca, give PSII centers with 40−80% of the oxygen evolution in the wildtype.[58] In addition, the S_2 state multiline EPR signal was similar in the wildtype and the Gln mutant. It thus seems clear that D1-Glu189 can be displaced from its site without major inhibitory effects of either activity or spectral properties.

The existence of the high affinity site for methanol is here proposed for the first time. Consequently, there are few discussions dealing with this site in the literature. However, both in the channel study by Ho and Styring[20] and in the spectroscopic analysis by Su et al.[21] methanol access to several Mn ions was discussed, mainly in structural terms. In both studies, Mn_A was discussed as a methanol binding site (Figure 6). Su et al. (Figure 8 in ref 21) pointed out that Mn_A has three potential coordination sites for methanol in the Siegbahn structure, the two OH-ligands and the D1-Asp170 ligand, and indicated that the ESEEM data from Force et al.[18] favored displacement of an OH ligand.[b] Potentially this could be the high affinity site.

If the above analysis is correct, the different ESEEM data sets from Åhrling et al.[19,35] and Force et al.[18] reflect methanol binding to different Mn ions. This can be rationalized following a discussion by Åhrling et al.[35] where it was concluded that the methanol binding studied in refs 19 and 35 involved a so-called narrow form of the S_2 state multiline EPR signal, while the methanol binding studied in ref 18 involved a broader form. Methanol binding to the low affinity site leads to the narrow form of the S_2 multiline EPR signal which we studied here (Figure 4). This we assign to methanol binding at Mn_D (affecting the $S_2Y_Z^\bullet$ EPR signal). In contrast, according to ref 35, the overall shape of the multiline EPR signal is not affected by methanol binding to the site studied by ESEEM in ref 18. This would then be the case when methanol binds to the high affinity site (affecting the $S_1Y_Z^\bullet$ EPR signal), and it is thus tempting to suggest that this site involves coordination to an OH site on Mn_A.

CONCLUSIONS

We have described methanol binding data to PSII in the S_2 state of the OEC. The data indicate the existence of two binding sites for methanol, one high and one low affinity site. The high affinity site is observable at least in the S_1 and S_2 states (so far not observed in the S_3 and S_0 states), while the low affinity site seems to be available in all S-states. The two sites are tentatively assigned to different Mn ions in the $CaMn_4$ cluster. We propose that the high affinity site reflects methanol displacement of an OH ligand to Mn_A ,while the low affinity site involves methanol displacement of the carboxy-group from D1-Glu189.

AUTHOR INFORMATION

Corresponding Author

*Telephone: +46 18 471 6580; fax: +46 471 6844; e-mail: stenbjorn.styring@kemi.uu.se.

Funding

The Swedish Energy Agency, the Knut and Alice Wallenberg Foundation, The EU program SOLAR-H2 (EU Contract 212508) and the Nordic Energy Research Program 06-Hydr-C13 are gratefully acknowledged for financial support.

Notes

The authors declare no competing financial interest.

ABBREVATIONS

Car, carotenoid; Chl, chlorophyll; Cytb_{559}, cytochrome b_{559}; D1 and D2, the core protein subunits in PSII; DMSO, dimethylsulfoxide; EPR, electron paramagnetic resonance; D1-His190, histidine 190 on the D1 protein that participates in hydrogen bonding to Y_Z; MES, 2-[*N*-morpholino] ethanesulfonic acid; NIR, near-infrared (here 830 nm); OEC, oxygen evolving complex consisting of the $CaMn_4$ cluster and surrounding amino acid ligands including Y_Z; P_{680}, primary electron donor chlorophylls in PSII; P*p*BQ, phenyl-*p*-benzoquinone; PSII, photosystem II; Pheo, pheo-phytin acceptor in PSII; Q_A and Q_B, primary and secondary plastoquinone acceptors of PSII; S states, intermediates in the cyclic turnover of the OEC; Y_Z, tyrosine 161 on the D1 protein

ADDITIONAL NOTES

[a]It has been suggested that this can be done by utilizing a pre-illumination at higher temperature (>77 K) to relocate a proton before the induction of the split $S_2Y_Z^\bullet$ signal.[29,36] Note here also that a backward electron transfer to produce the $S_1Y_Z^\bullet$ state is nevertheless possible since the reduction of the $CaMn_4$ cluster upon Y_Z oxidation lowers its charge, making the $Y_Z^\bullet$ − D1-His190$^+$ pair stably formed.[36]

[b]One cannot completely rule out the option of methanol displacing the Mn_A ligand D1-Asp170. This amino acid can, in analogy to D1-Glu189, be replaced by, e.g., Arg, Ile, Leu, and Val without completely losing the O_2 evolving capacity.[59,60] However, in the analysis by Su et al.,[21] displacement of D1-Asp170 was favored by neither the Force et al.[18] nor the Åhrling et al.[19] ESEEM data.

REFERENCES

(1) Nelson, N., and Yocum, C. F. (2006) Structure and function of photosystems I and II. *Annu. Rev. Plant Biol. 57*, 521−565.

(2) Goussias, C., Boussac, A., and Rutherford, A. W. (2002) Photosystem II and photosynthetic oxidation of water: an overview. *Philos. Trans. R. Soc. London, Ser. B 357*, 1369−1381.

(3) Rappaport, F., and Diner, B. A. (2008) Primary photochemistry and energetics leading to the oxidation of the (Mn)4Ca cluster and to the evolution of molecular oxygen in Photosystem II. *Coord. Chem. Rev. 252*, 259−272.

(4) Umena, Y., Kawakami, K., Shen, J.-R., and Kamiya, N. (2011) Crystal structure of oxygen-evolving photosystem II at a resolution of 1.9 Å. *Nature 473*, 55−60.

(5) Messinger, J., and Renger, G. (2008) Photosynthetic water splitting, In *Primary Processes of Photosynthesis - Part 2* (Renger, G., Ed.) pp 291−349, RSC Publishing, Cambridge.

(6) McEvoy, J. P., and Brudvig, G. W. (2006) Water-splitting chemistry of photosystem II. *Chem. Rev. 106*, 4455−4483.

(7) Dau, H., and Haumann, M. (2008) The manganese complex of photosystem II in its reaction cycle—Basic framework and possible realization at the atomic level. *Coord. Chem. Rev. 252*, 273−295.

(8) Diner, B. A., and Britt, R. D. (2005) The redox-active tyrosines Y_Z and Y_D, In *The Light-Driven Water:Plastoquinone Oxido-Reductase in Photosynthesis, Advances in Photosynthesis and Respiration* (Wydrzynski, T., and Satoh, K., Eds.) pp 206−233, Springer, Dordrecht.

(9) Mamedov, F., Sayre, R. T., and Styring, S. (1998) Involvement of histidine 190 on the D1 protein in electron/proton transfer reactions on the donor side of photosystem II. *Biochemistry 37*, 14245−14256.

(10) Hays, A. M. A., Vassiliev, I. R., Golbeck, J. H., and Debus, R. J. (1998) Role of D1-His190 in proton-coupled electron transfer reactions in photosystem II: A chemical complementation study. *Biochemistry 37*, 11352−11365.

(11) Styring, S., Sjöholm, J., and Mamedov, F. (2012) Two tyrosines that changed the world: Interfacing the oxidizing power of photochemistry to water splitting in photosystem II. *Biochim. Biophys. Acta 1817*, 76−87.

(12) Havelius, K. G. V., Sjöholm, J., Ho, F., Mamedov, F., and Styring, S. (2010) Metalloradical EPR signals from the $Y_Z^{\bullet}$S-state intermediates in photosystem II. *Appl. Magn. Reson. 37*, 151−176.

(13) Petrouleas, V., Koulougliotis, D., and Ioannidis, N. (2005) Trapping of metalloradical intermediates of the S-states at liquid helium temperatures. Overview of the phenomenology and mechanistic implications. *Biochemistry 44*, 6723−6728.

(14) Styring, S., and Rutherford, A. W. (1988) Deactivation kinetics and temperature-dependence of the S-state transitions in the oxygen-evolving system of photosystem II measured by EPR spectroscopy. *Biochim. Biophys. Acta 933*, 378−387.

(15) McConnell, I. (2008) Substrate water binding and oxidation in photosystem II. *Photosynth. Res. 98*, 261−276.

(16) Debus, R. J. (1992) The manganese and calcium ions of photosynthetic oxygen evolution. *Biochim. Biophys. Acta 1102*, 269−352.

(17) Hillier, W., and Messinger, J. (2005) Mechanism of photosynthetic oxygen production, In *The Light-Driven Water:Plastoquinone Oxido-Reductase in Photosynthesis, Advances in Photosynthesis and Respiration* (Wydrzynski, T., and Satoh, K., Eds.) pp 267−608, Springer, Dordrecht.

(18) Force, D. A., Randall, D. W., Lorigan, G. A., Clemens, K. L., and Britt, R. D. (1998) ESEEM studies of alcohol binding to the manganese cluster of the oxygen evolving complex of photosystem II. *J. Am. Chem. Soc. 120*, 13321−13333.

(19) Åhrling, K. A., Evans, M. C. W., Nugent, J. H. A., Ball, R. J., and Pace, R. J. (2006) ESEEM studies of substrate water and small alcohol binding to the oxygen-evolving complex of photosystem II during functional turnover. *Biochemistry 45*, 7069−7082.

(20) Ho, F. M., and Styring, S. (2008) Access channels and methanol binding site to the $CaMn_4$ cluster in Photosystem II based on solvent accessibility simulations, with implications for substrate water access. *Biochim. Biophys. Acta 1777*, 140−153.

(21) Su, J.-H., Cox, N., Ames, W., Pantazis, D. A., Rapatskiy, L., Lohmiller, T., Kulik, L. V., Dorlet, P., Rutherford, A. W., Neese, F., Boussac, A., Lubitz, W., and Messinger, J. (2011) The electronic structures of the S_2 states of the oxygen-evolving complexes of photosystem II in plants and cyanobacteria in the presence and absence of methanol. *Biochim. Biophys. Acta 1807*, 829−840.

(22) Su, J. H., Havelius, K. G. V., Mamedov, F., Ho, F. M., and Styring, S. (2006) Split EPR signals from photosystem II are modified by methanol, reflecting S state-dependent binding and alterations in the magnetic coupling in the $CaMn_4$ cluster. *Biochemistry 45*, 7617−7627.

(23) Deak, Z., Peterson, S., Geijer, P., Ahrling, K. A., and Styring, S. (1999) Methanol modification of the electron paramagnetic resonance signals from the S(0) and S(2) states of the water-oxidizing complex of photosystem II. *Biochim. Biophys. Acta 1412*, 240−249.

(24) Berthold, D. A., Babcock, G. T., and Yocum, C. F. (1981) A highly resolved, oxygen-evolving photosystem II preparation from spinach thylakoid membranes. *FEBS Lett. 134*, 231−234.

(25) Völker, M., Ono, T., Inoue, Y., and Renger, G. (1985) Effect of trypsin on PS II particles: Correlation between Hill-activity, Mn-abundance and peptide pattern. *Biochim. Biophys. Acta 806*, 25−34.

(26) Arnon, D. I. (1949) Copper enzymes in isolated chloroplasts. Polyphenoloxidase in *Beta Vulgaris*. *Plant Physiology 24*, 1−15.

(27) Styring, S., and Rutherford, A. W. (1987) In the oxygen-evolving complex of photosystem II the S_0 state is oxidized to the S_1 state by D^+ (Signal-II_{slow}). *Biochemistry 26*, 2401−2405.

(28) Cox, N., Pantazis, D. A., Neese, F., and Lubitz, W. (2013) Biological water oxidation. *Acc. Chem. Res.*, DOI: 10.1021/ar3003249.

(29) Ioannidis, N., Zahariou, G., and Petrouleas, V. (2006) Trapping of the S_2 to S_3 state intermediate of the oxygen-evolving complex of photosystem II. *Biochemistry 45*, 6252−6259.

(30) Havelius, K. G. V., Su, J. H., Feyziyev, Y., Mamedov, F., and Styring, S. (2006) Spectral resolution of the split EPR signals induced by illumination at 5 K from the S_1, S_3, and S_0 states in photosystem II. *Biochemistry 45*, 9279−9290.

(31) Koulougliotis, D., Shen, J. R., Ioannidis, N., and Petrouleas, V. (2003) Near-IR irradiation of the S_2 state of the water oxidizing complex of photosystem II at liquid helium temperatures produces the metalloradical intermediate attributed to $S_1Y_Z^{\bullet}$. *Biochemistry 42*, 3045−3053.

(32) Zhang, C., Boussac, A., and Rutherford, A. W. (2004) Low-temperature electron transfer in photosystem II: a tyrosyl radical and semiquinone charge pair. *Biochemistry 43*, 13787−13795.

(33) Zhang, C., and Styring, S. (2003) Formation of split electron paramagnetic resonance signals in photosystem II suggests that $tyrosine_Z$ can be photooxidized at 5 K in the S_0 and S_1 states of the oxygen-evolving complex. *Biochemistry 42*, 8066−8076.

(34) Havelius, K. G. V., Su, J.-H., Han, G., Mamedov, F., Ho, F. M., and Styring, S. (2011) The formation of the split EPR signal from the S_3 state of Photosystem II does not involve primary charge separation. *Biochim. Biophys. Acta 1807*, 11−21.

(35) Åhrling, K. A., Evans, M. C. W., Nugent, J. H. A., and Pace, R. J. (2004) The two forms of the S_2 state multiline signal in photosystem II: effect of methanol and ethanol. *Biochimica et Biophysica Acta (BBA) - Bioenergetics 1656*, 66−77.

(36) Sjöholm, J., Styring, S., Havelius, K. G. V., and Ho, F. M. (2012) Visible light induction of an EPR split signal in photosystem II in the S_2 state reveals the importance of charges in the oxygen evolving center during catalysis: a unifying model. *Biochemistry 51*, 2054−2064.

(37) Yamauchi, T., Mino, H., Matsukawa, T., Kawamori, A., and Ono, T.-a. (1997) Parallel polarization electron paramagnetic resonance studies of the S_1-state manganese cluster in the photosynthetic oxygen-evolving system. *Biochemistry 36*, 7520−7526.

(38) Pace, R. J., Smith, P., Bramley, R., and Stehlik, D. (1991) EPR saturation and temperature dependence studies on signals from the oxygen-evolving centre of photosystem II. *Biochim. Biophys. Acta 1058*, 161−170.

(39) Åhrling, K. A., Peterson, S., and Styring, S. (1998) The S_0 state EPR signal from the Mn cluster in photosystem II arises from an isolated S = 1/2 ground state. *Biochemistry 37*, 8115−8120.
(40) Kulik, L. V., Lubitz, W., and Messinger, J. (2005) Electron spin−lattice relaxation of the S_0 state of the oxygen-evolving complex in photosystem II and of dinuclear manganese model complexes. *Biochemistry 44*, 9368−9374.
(41) Lorigan, G. A., and Britt, R. D. (1994) Temperature-dependent pulsed electron paramagnetic resonance studies of the S_2 state multiline signal of the photosynthetic oxygen-evolving complex. *Biochemistry 33*, 12072−12076.
(42) Koulougliotis, D., Teutloff, C., Sanakis, Y., Lubitz, W., and Petrouleas, V. (2004) The S_1Y_Z metalloradical intermediate in photosystem II: an X- and W-band EPR study. *Phys. Chem. Chem. Phys. 6*, 4859−4863.
(43) Junge, W., Haumann, M., Ahlbrink, R., Mulkidjanian, A., and Clausen, J. (2002) Electrostatics and proton transfer in photosynthetic water oxidation. *Philos. Trans. R. Soc. London, Ser. B 357*, 1407−1417.
(44) Rappaport, F., Blanchard-Desce, M., and Lavergne, J. (1994) Kinetics of electron transfer and electrochromic change during the redox transitions of the photosynthetic oxygen-evolving complex. *Biochim. Biophys. Acta 1184*, 178−192.
(45) Ahlbrink, R., Haumann, M., Cherepanov, D., Bogershausen, O., Mulkidjanian, A., and Junge, W. (1998) Function of tyrosine Z in water oxidation by photosystem II: electrostatical promotor instead of hydrogen abstractor. *Biochemistry 37*, 1131−1142.
(46) Dau, H., and Haumann, M. (2007) Eight steps preceding O-O bond formation in oxygenic photosynthesis - a basic reaction cycle of the photosystem II manganese complex. *Biochim. Biophys. Acta 1767*, 472−483.
(47) Nöring, B., Shevela, D., Renger, G., and Messinger, J. (2008) Effects of methanol on the S_i-state transitions in photosynthetic water-splitting. *Photosynth. Res. 98*, 251−260.
(48) Ioannidis, N., and Petrouleas, V. (2000) Electron paramagnetic resonance signals from the S_3 state of the oxygen-evolving complex. A broadened radical signal induced by low-temperature near-infrared light illumination. *Biochemistry 39*, 5246−5254.
(49) Matsukawa, T., Mino, H., Yoneda, D., and Kawamori, A. (1999) Dual-mode EPR study of new signals from the S_3-state of oxygen-evolving complex in photosystem II. *Biochemistry 38*, 4072−4077.
(50) Loll, B., Kern, J., Saenger, W., Zouni, A., and Biesiadka, J. (2005) Towards complete cofactor arrangement in the 3.0 Å resolution structure of photosystem II. *Nature 438*, 1040−1044.
(51) Haumann, M., Muller, C., Liebisch, P., Iuzzolino, L., Dittmer, J., Grabolle, M., Neisius, T., Meyer-Klaucke, W., and Dau, H. (2005) Structural and oxidation state changes of the photosystem II manganese complex in four transitions of the water oxidation cycle ($S_0 \rightarrow S_1$, $S_1 \rightarrow S_2$, $S_2 \rightarrow S_3$, and $S_{3,4} \rightarrow S_0$) characterized by X-ray absorption spectroscopy at 20 K and room temperature. *Biochemistry 44*, 1894−1908.
(52) Messinger, J., Robblee, J. H., Bergmann, U., Fernandez, C., Glatzel, P., Visser, H., Cinco, R. M., McFarlane, K. L., Bellacchio, E., Pizarro, S. A., Cramer, S. P., Sauer, K., Klein, M. P., and Yachandra, V. K. (2001) Absence of Mn-centered oxidation in the $S_2 \rightarrow S_3$ transition: Implications for the mechanism of photosynthetic water oxidation. *J. Am. Chem. Soc. 123*, 7804−7820.
(53) Kulik, L. V., Epel, B., Lubitz, W., and Messinger, J. (2007) Electronic structure of the Mn_4O_xCa cluster in the S_0 and S_2 states of the oxygen-evolving complex of photosystem II based on pulse ^{55}Mn-ENDOR and EPR spectroscopy. *J. Am. Chem. Soc. 129*, 13421−13435.
(54) Ames, W., Pantazis, D. A., Krewald, V., Cox, N., Messinger, J., Lubitz, W., and Neese, F. (2011) Theoretical evaluation of structural models of the S_2 state in the oxygen evolving complex of photosystem II: protonation states and magnetic interactions. *J. Am. Chem. Soc. 133*, 19743−19757.
(55) Pantazis, D. A., Orio, M., Petrenko, T., Zein, S., Lubitz, W., Messinger, J., and Neese, F. (2009) Structure of the oxygen-evolving complex of photosystem II: information on the S_2 state through quantum chemical calculation of its magnetic properties. *Phys. Chem. Chem. Phys. 11*, 6788−6798.
(56) Asada, M., Nagashima, H., Koua, F. H. M., Shen, J.-R., Kawamori, A., and Mino, H. (2013) Electronic structure of S_2 state of the oxygen-evolving complex of photosystem II studied by PELDOR. *Biochim. Biophys. Acta 1827*, 438−445.
(57) Siegbahn, P. E. M. (2009) Structures and energetics for O_2 formation in photosystem II. *Acc. Chem. Res. 42*, 1871−1880.
(58) Debus, R. J., Campbell, K. A., Pham, D. P., Hays, A. M. A., and Britt, R. D. (2000) Glutamate 189 of the D1 polypeptide modulates the magnetic and redox properties of the manganese cluster and tyrosine Y_Z in photosystem II. *Biochemistry 39*, 6275−6287.
(59) Chu, H.-A., Nguyen, A. P., and Debus, R. J. (1995) Amino acid residues that influence the binding of manganese or calcium to photosystem II. 1. The lumenal interhelical domains of the D1 polypeptide. *Biochemistry 34*, 5839−5858.
(60) Nixon, P. J., and Diner, B. A. (1992) Aspartate 170 of the photosystem II reaction center polypeptide D1 is involved in the assembly of the oxygen-evolving manganese cluster. *Biochemistry 31*, 942−948.